

The Application of Dyadic Wavelet in the RS Building Image Edge Detection*

Qin Qiming Author1

Laboratory of Remote Sensing and GIS, Peking University, Beijing 100871, China;

qmqin@pku.edu.cn

Wang Wenjun Author2

Department of Communication Engineering, Yanshan University, Qinhuangdao, Heibei, 066004, China;

wwtingyan0662@sina.com

Chen Sijin Author3

Laboratory of Remote Sensing and GIS, Peking University, Beijing 100871, China;

dennis58220@263.net

Abstract: In the edge detection of RS building image, the useful detail losing and the spurious edge often appear. To solve the problem, we used the dyadic wavelet to detect the edge of surface features by combining the edge detecting with the multi-resolution analyzing of the wavelet transform. Via the dyadic wavelet decomposing, we obtained the RS building image of a certain appropriate scale, and figured out the edge data of the plane and the upright directions respectively, then worked out the grads vector module of the surface features, at last by tracing them we got the edge data of the buildings therefore builded the RS image which obtained the checked edge. This method can depress the effect of noise and examine exactly the edge data of the building object by rule and line. With an experiment of RS building image, we certificated the feasibility of the application of dyadic wavelet in the RS building image edge detection.

Keywords: Dyadic Wavelet, Buildings, Remote Sensing Image, Edge Detection and Tracking, Object Recognition.

1. Introduction

In the RS building image, because the buildings are collocated un-orderly, the conventional filter methods often used the zero-crossing detection to examine the characteristic, but they often obtained some spurious edge when they faced the special details. Here we

* Project (No. 40071061) supported by NSFC

introduced dyadic wavelet transform to deal with the RS building image.

The wavelet analysis is a relatively new image tool which is rapidly developed from the Fourier transform, it has favorable localized character in the both spatial domain and frequency domain. The wavelet analysis consists of orthogonal wavelet, biorthogonal wavelet, dyadic wavelet, discrete wavelet and wavelet packets. Here we introduced dyadic wavelet to do edge detection of the RS building image.

Dyadic wavelet [1] is a kind of wavelet between continuous wavelet and discrete wavelet, it has discrete scale parameters and continuous parameters in the spatial domain. So it has the same spatial-frequency covariational character as continuous wavelet which makes it important for the signal oddity detection and the edge detection.

The edges in an image can be divided into two groups: the step-edges and the roof-edges [2]. The gray levels of the image pixels on the two sides of the step-edge are totally different. The roof-edges are the points whose gray levels are from the increasing to the decreasing. It can be seen that the second order derivatives of the step-edges are zero-crossing and the second order derivatives of the roof-edges are the extrema. In order to use dyadic wavelet in the edge detection, the wavelet is required to have linear

displacement, in other words, dyadic wavelet must be zero-symmetrical. Therefore we could construct the zero-antisymmetrical and the zero-symmetrical dyadic wavelets[3].

If $\varphi(t)$ is a mother dyadic wavelet, $H(\omega)$ is the creating-atom, N is a random positive integer, array

$$(a_1, a_2, \dots, a_N) \text{ satisfies } \sum_{k=1}^N |a_k| < 1, \text{ we denote}$$

${}_s\psi(t) \in L^2(R)$ as a zero-antisymmetrical dyadic wavelet, then ${}_s\psi(t)$ satisfies

$${}_s\hat{\psi}(2\omega) = {}_sG(\omega)\hat{\varphi}(\omega) \quad (1)$$

where ${}_sG(\omega)$ is a high-pass filter for the structure of a zero-antisymmetrical dyadic wavelet

$${}_sG(\omega) = i \operatorname{sgn}(\omega) \left(1 + \sum_{k=1}^N a_N \cos k\omega\right) \sqrt{1 - |H(\omega)|^2} \quad (2)$$

If $\varphi(t)$ is a mother dyadic wavelet, $H(\omega)$ is the creating-atom, N is a random positive integer, array (a_1, a_2, \dots, a_N) satisfies $\sum_{k=1}^N |a_k| < 1$, we denote ${}_c\psi(t) \in L^2(R)$ as a zero-symmetrical dyadic wavelet, then ${}_c\psi(t)$ satisfies

$${}_c\hat{\psi}(2\omega) = {}_cG(\omega)\hat{\varphi}(\omega) \quad (3)$$

where ${}_cG(\omega)$ is a high-pass filter for the structure of a zero-symmetrical dyadic wavelet

$${}_cG(\omega) = \left(1 + \sum_{k=1}^N a_N \cos k\omega\right) \sqrt{1 - |H(\omega)|^2} \quad (4)$$

Therefore we get two filters for the structures of dyadic wavelets ${}_sG(\omega)$ and ${}_cG(\omega)$, where ${}_sG(\omega)$

is an odd function, ${}_cG(\omega)$ is an even function,

$${}_sG(\omega) = \sum_{n \in \mathbb{Z}} {}_s g_n e^{-in\omega} \quad (5)$$

$${}_cG(\omega) = \sum_{n \in \mathbb{Z}} {}_c g_n e^{-in\omega} \quad (6)$$

2. Edge Detection and Tracking of Images

In the dyadic wavelet decomposition of an image we should determine three filters: where $H(\omega)$ is the creating-atom of the mother dyadic wavelet, $G(\omega)$ is just defined in Eq.(5) and Eq.(6), $L(\omega)$ is a low-pass filter such that

$$L(\omega) = \frac{1}{\sqrt{2}} \left(1 + \sum_{k=1}^N b_k \cos k\omega\right) \sqrt{1 + |H(\omega)|^2} \quad (7)$$

where array (b_1, b_2, \dots, b_N) satisfies $\sum_{k=1}^N |b_k| < 1$. Then

we could define $\hat{\varphi}(2w), \hat{\psi}(2w), \hat{\xi}(2w)$

$$\begin{aligned} \hat{\varphi}(2w) &= H(w)\hat{\varphi}(w) \\ {}_c\hat{\psi}(2w) &= {}_cG(w)\hat{\varphi}(w), {}_s\hat{\psi}(2w) = {}_sG(w)\hat{\varphi}(w) \\ \hat{\xi}(2w) &= L(w)\hat{\varphi}(w) \end{aligned} \quad (8)$$

At last we obtain the smooth function in two dimensions:

$$\varphi(x, y) = \varphi(x)\varphi(y) \quad (9)$$

$$\hat{\varphi}(\omega_x, \omega_y) = \hat{\varphi}(\omega_x)\hat{\varphi}(\omega_y) \quad (10)$$

and the zero-antisymmetrical functions in two dimensions:

$${}_s\psi^1(x, y) = {}_s\psi(x)\xi(y) \quad (11)$$

$${}_s\psi^2(x, y) = {}_s\psi(y)\xi(x) \quad (12)$$

and the zero-symmetrical functions in two dimensions:

$${}_c\psi^1(x, y) = {}_c\psi(x)\xi(y) \quad (13)$$

$${}_c\psi^2(x, y) = {}_c\psi(y)\xi(x) \quad (14)$$

The figure of dyadic wavelet decomposition in two dimensions [4] is:

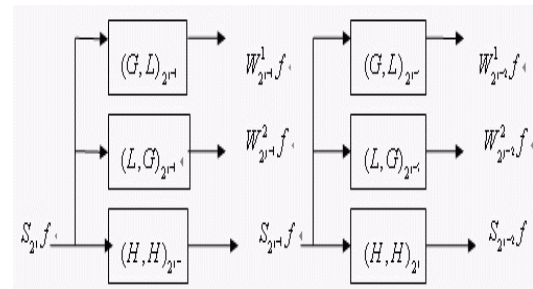


Fig1 Dyadic Wavelet Decomposition in Two Levels

where $S_{2^i} f_i(x, y)$ is the portion which is smoothed

both in the plane and upright directions after being decomposed in the level j , $W_{2^j}^1 f(x,y)$, $W_{2^j}^2 f(x,y)$ are the edge information in the plane and upright directions respectively. In each scale, edge information expresses the local module maxima which mean the gradient vector module maxima. The gradient vector module is $M_{2^j} f(x,y) = \sqrt{(W_{2^j}^1 f)^2 + (W_{2^j}^2 f)^2}$, and

$$A_{2^j} f(x,y) = \arctan\left(\frac{W_{2^j}^2 f}{W_{2^j}^1 f}\right)$$
 is the gradient vector angle.

So it is clear that edge information is the points which are the gradient module maxima in the gradient vector angle direction.

In case of a building image after pretreatment $f(x,y)$ (Fig.2) we used dyadic wavelet to decompose in one level ($j=1$), after computing

$$S_2 f(x,y) = \sum_{l \in Z} \sum_{k \in Z} h_l h_k S f(x-l, y-k)$$
, we got the smooth portion of the image (Fig.3).



Fig.2. The Building Image **Fig.3. The Smoothed Image**

After computing

$$W_2^1 f(x,y) = \sum_{l \in Z} \sum_{k \in Z} g_l l_k S f(x-l, y-k),$$

$$W_2^2 f(x,y) = \sum_{l \in Z} \sum_{k \in Z} l_l g_k S f(x-l, y-k),$$
 we got the

images depicting the edge information of the plane direction (Fig.4) and the upright direction (Fig.5) respectively.

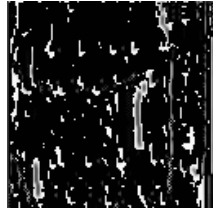


Fig.4. The Plane Edge Information

Fig.5. The Upright Edge Information

By computing the gradient vector module

$M_{2^j} f(x,y) = \sqrt{(W_{2^j}^1 f)^2 + (W_{2^j}^2 f)^2}$, we got the edge of the image (Fig.6).



Fig.6. The Edge image

Now we had got the edges of an image by computing the gradient vector module of some certain scale after dyadic wavelet decomposition. But this time the edges contained some inconsecutive points and spurious edges. So the edge tracking is needed. The edge tracking is to connect the discontinuous edge points together to a close boundary. The process fills up the clearance which is produced by noise and the shadow. Here we proposed a new best-path method to track the edges. The method is:

1) Mark the coordinate $A(x,y)$ of the edge point A

which is in the top left corner of the gradient vector module image, then use A as the center open a window whose size is 30×30 . If both coordinates of A are less than the default threshold (such as 30), then let the smaller of x and y as the radius of the window, and mark A.

2) In the window, from the plane direction, ascertain counter-clockwise the detected edge point which is nearest the center and not marked. Then let the point as the center B of the next window, if A and B are 8-adjacent, then mark B, otherwise, we should ascertain the best path between A and B.

3) The best path between A and B is ascertained in this step. The path should be along the gradient direction of A and B, and the number of the path points should be the least. Then mark the path points as A and B.

4) After ascertaining B, let B as the start point, repeat 1),2),3) until goes back to A. Therefore we get the whole edge.

4. The Experiment of Edge Detection and Discussion

Here we use the dyadic wavelet to detect the edges of building images in various scales to find a best scale for the detection. The original building images are Fig.7, Fig.8, Fig.9.

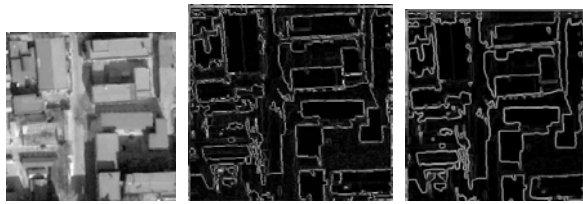


Fig.7. The Building Image Fig.7-1 Fig.7-2

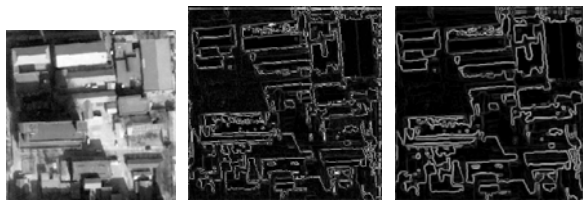


Fig.8 The Building Image Fig.8-1 Fig.8-2

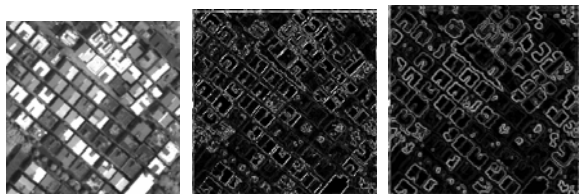


Fig.9 The Building Image Fig.9-1 Fig.9-2

From the building images Fig.7, Fig.8 and Fig.9, different building images appear different character, Fig.7-1, 8-1, and 9-1 are the gradient vector module of original image Fig.7, Fig.8, Fig.9 after dyadic wavelet decomposition for one layer respectively. Since dyadic wavelet has discrete scale parameters and continuous parameters in the spatial domain, when dyadic wavelet decompose the image for j levels, the scale is 2^j , so the outcomes of different scales are the embodiment of multi-resolution. From the decomposed image, the resolution is decrease when the scale is increase, at the same time, noise is restrained apparently. Meanwhile, some detail is lost in result of the increasing scales, therefore lead the detected edge incomplete and the position of the edge inaccurate. Moreover when the scale is small, the influence of noise is undeniable. So it is valuable to get the suitable scale which not only restrains noise effectively but also detects the edge accurately. Here we decomposed the image for two layers (Fig.7-2, Fig.8-2, Fig.9-2), and used the method mentioned above to track the edge (Fig.7-3, Fig.8-3, Fig.

9-3) respectively.

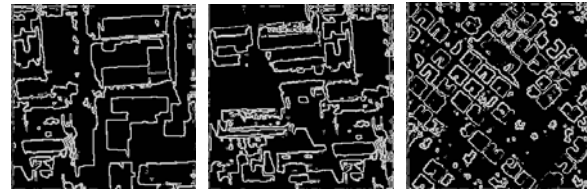


Fig.7-3 Fig.8-3 Fig.9-3

From the result of the experiment, we found that it was feasible for dyadic wavelet to detect the edges of RS building images and solve problem of both straining noise and localizing edges. Especially, some details can be detected accurately, and there is almost no spurious edge. The key of the application of this method is to choose a most suitable scale according to the character of the different image in order to detect the edge accurately without losing essential detail and restrain noise as well. In a certain suitable scale, dyadic wavelet can detect the specific diversification of the image edge character, and with our edge tracking method, we can connect the edges into a close curve which provides the foundation for the further researches such as object recognition.

References

- [1] Peng Yu-hua, Wavelet transform and engineering application, Science press, p.33
- [2] Liu Liudi, Liu Mingqi, Practical digital image processing, Beijing institute of technology press, p.180
- [3] Xu Chuanxiang, Shi Qingyun and Cheng Minde, Zero-symmetrical and zero-antisymmetrical dyadic wavelet and its application to edge detection, *China journal of image and graphics*, Vol.1, No.1, May, pp4-11, 1996
- [4] Stephane Mallat, Sifen Zhong Characterization of Signals from Multiscale Edges. *Trans. Patt. Anal. Machine Intell.*, Vol. 14, No.7, pp. 710-732. 1992.